

## Understanding the structural properties of zeolites for isobutane alkylation based on adsorption/diffusion behaviors

Bihong Li <sup>a,1</sup>, Pan Huang <sup>a,1</sup>, Piao Cao <sup>a</sup>, Weiqun Gao <sup>a</sup>, Weizhong Zheng <sup>a,\*\*</sup>, Cheng Lian <sup>a</sup>, Weizhen Sun <sup>a,\*</sup>, Ling Zhao <sup>a,b</sup>

<sup>a</sup> State Key Laboratory of Chemical Engineering, School of Chemical Engineering, East China University of Science and Technology, Shanghai, 200237, China

<sup>b</sup> School of Chemistry & Chemical Engineering, Xinjiang University, Urumqi, 830046, China



### ARTICLE INFO

**Keywords:**  
Isobutane alkylation  
Zeolite  
Molecular simulations  
Adsorption  
Diffusion

### ABSTRACT

Although zeolites are well-accepted as environmentally friendly catalysts for the isobutane alkylation, the structure-performance relationship between C4 reactants (isobutane and butene) and zeolites is less reported. Herein, the adsorption and diffusion behaviors of C4 reactants on zeolites with different topologies were investigated using configuration bias Monte Carlo (CBMC) and molecular dynamics (MD) simulations under experimental conditions in 348 K and 2.5 MPa. It is revealed that surface area, largest cavity diameter, and pore limiting diameter are the most relevant structural parameters for zeolites to determine the adsorption and diffusion of C4 reactants. In addition, the dimensions of the zeolitic channels can also affect the selectivity of isobutane to butene and the diffusion of C4 reactants, thereby affecting the process of isobutane alkylation reaction. This work can provide a good reference for the design of novel zeolites for isobutane alkylation.

### 1. Introduction

Alkylate is considered as an ideal gasoline blending component, which is produced from isobutane with light olefins in the presence of strong acids due to its high octane number, low vapor pressure, low sulfur content, and the absence of olefins and aromatic components [1, 2]. As a novel catalyst for isobutane alkylation, solid acids exhibit good initial activity, product selectivity, and ease of product separation, which makes the alkylation process more environmentally friendly than the liquid acid catalyst [3,4]. Solid acid catalysts include zeolites, metal halides, sulfated zirconia, mixed oxides, heteropolyacids, and acid resins [5]. Among these solid acid catalysts, zeolite is considered as a potential substitute due to its structural designability and acid adjustability, which has a good application prospect in the isobutane alkylation industry [6–8]. However, zeolite catalysts often suffer from rapid deactivation due to carbonaceous deposits and difficult regeneration, which limits their industrial application [9–11].

According to the carbonium ion mechanism of isobutane alkylation, the polar olefins, even at a low concentration, can be easily absorbed on the zeolite acid sites due to high polar zeolitic surface and strong

electrostatic zeolite pores [12–14]. The irreversible olefin adsorption results in olefin oligomerization, which can block the pores and channels, and further leads to the deactivation of zeolites [15,16]. Thus, the reduction of the olefin concentration around the acid sites and the olefin diffusion rate in zeolite pores is imperative to extending the zeolite lifetime. Many researchers are devoted to solving the problem by modifying the operation parameters and the physical-chemical properties of zeolites, including feed composition and zeolite topologies [17–19]. Corma et al. observed that the increased feed isoparaffin/olefin (I/O) ratio from 15 to 25 could improve the quality of alkylate using beta-zeolite at continuous alkylation process [20]. The high I/O ratio is usually needed to inhibit the oligomerization of butene, which is a very important factor for zeolite-catalyzed alkylation [21,22]. A study of the effect on the topologies with different pore sizes by Chu and Chester [23] showed that ZSM-5 was inactive for the alkylation, while the desirable trimethylpentanes (TMPs) selectivity appeared to be controlled by the diffusion in the medium-pore ZSM-5 zeolite and large-pore REHY zeolite. Mota et al. [24] researched the effect of different dimensional channels on the isobutane alkylation. The authors found that beta-zeolite with uniform channels was superior to USY

\* Corresponding author.

\*\* Corresponding author.

E-mail addresses: [wzzheng@ecust.edu.cn](mailto:wzzheng@ecust.edu.cn) (W. Zheng), [sunwz@ecust.edu.cn](mailto:sunwz@ecust.edu.cn) (W. Sun).

<sup>1</sup> They contribute equally to this work.

zeolite in TMPs selectivity and catalytic lifetime because of the isobutane diffusion restriction in micropores. Corma et al. [25] found that three-dimensional (3D) pore structure zeolites are more conducive to diffusion than one-dimensional (1D) pore structure zeolites, which propagates the alkylation. Conversely, Yoo et al. [7] compared five 12-membered ring zeolites with different dimensional channels, concluding that 3D beta-zeolite and 1D ZSM-12 zeolite with linear channels and without connecting the huge supercage have less steric resistance than 3D USY and LTL zeolites, which promotes the formation of huge TMPs (2,2,4-TMP, 2,2,3-TMP) and inhibits the production of heavy hydrocarbons ( $C_9^+$ ). Hence, the adsorption and diffusion of C4 reactants (isobutane and butene) are dependent on the topologies of zeolites to a great extent, which plays a crucial role in determining the catalytic performance and lifetime of zeolites. Nevertheless, the mechanism of adsorption and diffusion behaviors of C4 reactants in zeolites is still unclear. It is difficult to correlate the adsorption and diffusion performance of C4 reactants and the structural features of zeolite catalysts, which hinders the screening of zeolites for isobutane alkylation.

Fortunately, molecular simulations, including Monte Carlo (MC) and molecular dynamics (MD) methods, are a promising way to determine the adsorptive and diffusive behaviors of adsorbates in zeolites, which can provide valuable information at a molecular level to correlate the structure-performance relationship. A series of researches have studied the adsorption and diffusion properties of a single component or binary mixture for alkanes and alkenes by using MC or MD simulations [26–28]. Whereas, only a few types of research focus on the adsorption and diffusion performance for the isobutane alkylation in zeolites. Zhang [29] et al. calculated the equilibrium adsorption capacities and self-diffusion coefficients of isobutane and 2-butene in Y-zeolite with different pore sizes by MC and MD methods, respectively. The authors found that the addition of mesopores can efficiently increase the uptake of isobutane and 2-butene around the acid sites and the diffusion rate of heavy hydrocarbons like  $C_{12}H_{26}$ . Cao et al. [30] studied the adsorption behaviors of C4 reactants in five zeolitic topologies, including BEA, FAU, LTL, MOR, and MTW, using CBMC simulations, and found that the selectivity of isobutane to butene was positively associated with the catalytic stability of zeolites, making the large-scale screening of C4 alkylation catalyst using MC simulation possible. However, the current calculation for C4 alkylation is only focused on several common zeolites. It is urgent to establish a structure-performance relationship for zeolites with a wide variety of topologies.

Herein, the aim of this work is to establish a structure-performance relationship between zeolite structures and the adsorption/diffusion behaviors of C4 reactants (isobutane and 1-butene) using CBMC and MD simulations. Specifically, the adsorption and diffusion properties of C4 reactants in 70 all-silica zeolites selected from the Structure Commission of the International Zeolite Association (SC-IZA) [31] were calculated, in which the adsorption uptake, adsorption selectivity, and diffusion coefficient of C4 reactants were analyzed. Furthermore, the influence of C4 feed composition on the adsorption and diffusion properties of C4 reactants was investigated and correlated with zeolite structures in detail. Finally, 12 zeolites that can adsorb both isobutane and 1-butene molecules were selected to further analyze the channel and pore effect on the adsorption and diffusion properties as well as their suitability for isobutane alkylation.

## 2. Methodology

### 2.1. Screening workflow

**Fig. 1** illustrates the workflow in three steps to screen zeolite structures for the calculation of the adsorption and diffusion of C4 reactants of isobutane alkylation. The structures of zeolite framework types were taken from the IZA database containing 243 fully ordered structures and 11 partially disordered ones (see **Fig. S1**). Initially, geometrical parameters of zeolites, including pore limiting diameter (PLD), largest

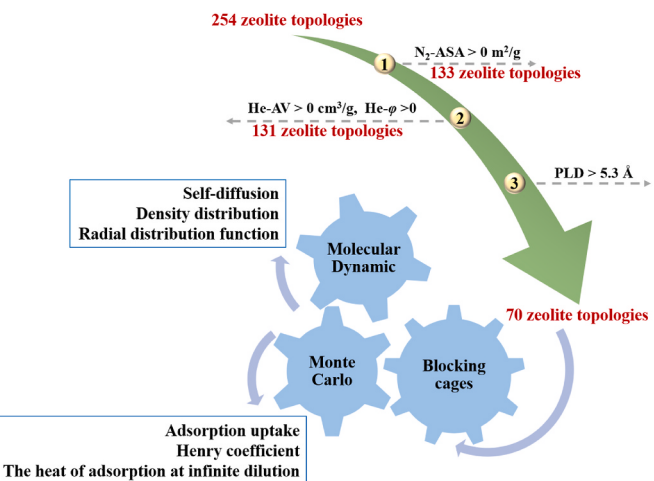


**Fig. 1.** Screening procedure for C4 reactants with molecular simulations from all-silica structures from the IZA database.

cavity diameter (LCD), accessible surface area (ASA), void fraction ( $\phi$ ), and accessible volume (AV), were calculated by Zeo++ software package [32]. Herein, the nitrogen ( $N_2$ , a radius of 1.8 nm) molecule and helium (He, a radius of 1.2 nm) molecule were used as probes to calculate ASA ( $N_2$ -ASA), AV (He-AV), and  $\phi$  (He- $\phi$ ), respectively. Note that ASA is considered as the theoretical surface area, which is usually used to evaluate the porosity of materials. 133 zeolites with ASA  $> 0 \text{ m}^2/\text{g}$  were selected (see Step 1). Moreover,  $\phi$  and AV also play important roles in measuring porosity. Thus, 131 zeolites out of 133 were found with  $\phi > 0$  and AV  $> 0$  (Step 2). PLD is defined as a circular gate that ensures the largest molecule freely diffuses through the porous zeolites without hindrance. As indicated in Step 3, considering the kinetic diameter of isobutane molecule (5.28 Å) and 1-butene molecule (4.31–4.94 Å), as listed in **Table S1**, the PLD  $> 5.3 \text{ \AA}$  was set as a screening metric, finally leaving 70 types of zeolites frameworks. Then, the adsorption and diffusion behaviors of the C4 reactants in the 70 zeolites frameworks were calculated by MC and MD simulations, respectively. The remaining zeolites probably have some isolated pores which can adsorb C4 reactants by MC simulations but are experimentally inaccessible [33]. In order to eliminate the influence of isolated pores, the Zeo++ package was used to block them (See the Supporting Information for details).

As mentioned above, CBMC simulations were performed to obtain the selective adsorption behaviors and determine the equilibrium spatial distribution of isobutane and 1-butene within the channels of 70 zeolite structures. The thermal properties containing Henry coefficient ( $K_H$ ) and isosteric heat of adsorption ( $Q_{st}$ ) were calculated under canonical (NVT) ensemble with the Widom particle-insertion method [34]. The diffusion behaviors of isobutane and 1-butene inside zeolites were investigated using MD simulations based on the equilibrium adsorption configurations of different systems obtained from MC simulations. Three feed I/O ratios, namely 1:1, 20:1, 40:1, were set to investigate the influence of feed composition change on the adsorption and diffusion behaviors into zeolites. All the simulations were conducted at 348 K and 2.5 MPa, corresponding to the practically experimental alkylation conditions [35].

### 2.2. Force field parameters

The isobutane and 1-butene mixtures were mimicked by the united-atom (UA) model, which treats  $\text{CH}_x$  groups as single, charge-less interaction sites (pseudo-atoms) [36]. The force field parameters of C4 reactants and zeolites were taken from the united atom force field which has been successfully applied in the simulations of hydrocarbons in zeolites [37–41]. The validation of the force field can be seen in the

**Supporting Information.** The interactions of the united atoms are divided into bonded and non-bonded contributions. The bonded potential includes bond stretching, bond bending, and torsion. The non-bonded potential is described by van der Waals (Lennard-Jones, L-J) and electrostatic (Coulombic) potential. Frameworks of the pure-silica zeolites were assumed to be rigid during the CBMC and MD simulations because of mechanical stability, which was widely used in the simulation, especially high-throughput simulation [42–44]. The potential parameters for C4 hydrocarbons and zeolites were listed in Table S2. In addition, the L-J parameters between adsorbents and adsorbates were calculated using Lorentz-Berthelot mixing rules.

### 2.3. Molecular simulation process

As dependent on pressure and temperature, the adsorbed amount of hydrocarbons in zeolites is generally calculated by grand-canonical Monte Carlo (GCMC) simulations [45]. However, the adsorbate is randomly inserted into the adsorbent in the form of the complete molecule, which may lead to the overlap of adsorbate molecules and a long calculation time [28]. Fortunately, the CBMC method combined with the GCMC simulation can realize the effective calculation, which allows the growth of a molecule atom by atom [46,47]. CBMC simulation was run for  $2 \times 10^5$  cycles for each system, with the initial  $1 \times 10^5$  cycles for equilibration and the last  $1 \times 10^5$  cycles for ensemble averages. Each cycle included  $N$  trial moves, including translation, rotation, reinsertion, swap, regrowth, and identity change.

For MD simulation, the leap-frog algorithm was used to integrate Newton's equations of motion under periodic boundary conditions [48]. The Nosé-Hoover thermostat was used to control the temperature of the system at 348 K [49,50]. Each MD simulation time was 20 ns, and the velocities were recorded every 1000 steps. The trajectory was generated every 1 ps for analysis. The L-J interactions were calculated with 12 Å cutoff and periodic boundary conditions were used in all three directions. CBMC simulations were implemented by the RASPA code [51] and MD simulations were performed by the GROMACS package [52].

### 2.4. Adsorption and diffusion metrics

The selectivity of isobutane to 1-butene ( $S_{iC4/C4=}$ ) and relative diffusion coefficient of isobutane to 1-butene ( $D_{iC4/C4=}$ ) as metrics were calculated to estimate the performance of all-silica zeolites for the structure-performance relationship between zeolites and C4 reactants. The metrics were defined as following equations.

$$S_{iC4/C4=} = \frac{x_{iC4}/x_{C4=}}{y_{iC4}/y_{C4=}} \quad (1)$$

$$D_{iC4/C4=} = D_{iC4}/D_{C4=} \quad (2)$$

where  $x_{iC4}$  and  $x_{C4=}$  represent the composition of component isobutane and 1-butene in adsorbed phase, respectively.  $y_{iC4}$  and  $y_{C4=}$  represent the composition of component isobutane and 1-butene bulk phase, respectively.  $D_{iC4}$  and  $D_{C4=}$  are self-diffusion coefficients ( $D_{self}$ ) of isobutane and 1-butene, respectively. The  $D_{self}$  was calculated according to Einstein equation [53].

$$D_i = \frac{1}{6} \lim_{t \rightarrow \infty} \frac{d}{dt} \langle [\vec{r}_i(t) - \vec{r}_i(0)]^2 \rangle \quad (3)$$

where  $\langle [\vec{r}_i(t) - \vec{r}_i(0)]^2 \rangle$  means the mean square displacement (MSD). The MSD is defined as the following Equation [54],

$$MSD = \langle \Delta |\vec{r}|^2 \rangle = \frac{1}{N} \langle \sum_{i=1}^N |\vec{r}_i(t) - \vec{r}_i(0)|^2 \rangle \propto \beta^\alpha \quad (4)$$

where  $\beta$  describes the type of motion of the molecules. Among the Equation (4), the  $D_{self}$  and  $\beta$  can be derived from the slope of MSD curves

as listed in Equations (5) and (6),

$$D_i = \frac{d(MSD)}{dt} \quad (5)$$

$$\beta = \frac{d \log(MSD)}{d \log(t)} \quad (6)$$

The slope of MSD curves was determined in the range of time intervals from 1500 ps to 6400 ps (see Fig. S2). Huang et al. considered that the nonlinear logarithm of MSD versus time is caused by the adsorption of guest molecules on the surface of zeolites, which usually intercepts the straight part to get the diffusion coefficient [43,55,56]. Thus, the  $D_{self}$  and  $\beta$  were obtained after taking linear fits for double logarithmic inset in Fig. S2. The correlation coefficient  $R^2$  lower than 0.95 of  $D_{self}$  was removed to ensure the reliability of data fitting. The definition is listed in the following Equation.

$$R^2 = r(y, \hat{y})^2 = \frac{\sum_i (\hat{y}_i - \bar{y})^2}{\sum_i (y_i - \bar{y})^2} \quad (7)$$

where  $r(y, \hat{y})^2$  is the proportion of variance in  $y$  explained by a linear function of  $x$ ,  $y_i$  is the observed value,  $\bar{y}$  is the average value, and  $\hat{y}_i$  is the predicted value. Unreliable data with  $R^2 < 0.95$  is removed.

The correlation between the adsorption capacity and diffusion coefficient of C4 reactants and the structural and thermal properties of zeolites was quantitated by Pearson correlation coefficients ( $\rho_{corr}$ ) [57],

$$\rho_{corr} = \frac{E[(X - \mu_X)(Y - \mu_Y)]}{\sigma_X \sigma_Y} \quad (8)$$

where  $\mu_X$  and  $\mu_Y$  are the mean of  $X$  and  $Y$ , respectively.  $\sigma_X$  and  $\sigma_Y$  are the standard deviation of  $X$  and  $Y$ , respectively.  $E$  is the expectation.

## 3. Results and discussion

### 3.1. Adsorption characteristics

The adsorption characteristics for guest molecules are mainly dependent on the structural and thermal properties of adsorbates. For the solid acid alkylation with zeolites as catalyst, the adsorption characteristics of C4 reactants in the zeolites are of critical importance to the alkylation quality and lifetime of zeolite catalyst [58]. Thus, the adsorption ability and the adsorption selectivity of isobutane to butene in the screened 70 types of zeolites at three feed ratios of I/O were initially computed by CBMC with the value listed in Table S3. To further figure out the relationship between adsorption characteristics of C4 reactants and the structural features of zeolites, the Pearson correlation coefficients ( $\rho_{corr}$ ) of isobutane and butene uptakes with six zeolite structures parameters (PLD, LCD,  $R_{PLD/LCD}$ ,  $\varphi$ , AV, and ASA) and a thermal parameter ( $Q_{st}$ ) were calculated at different feed ratios of I/O, as shown in Fig. 2. In terms of structural parameters, ASA, AV,  $\varphi$ , and LCD are positively correlated with the adsorption capacity of C4 reactants, while  $R_{PLD/LCD}$  shows a negative correlation. PLD has a positive effect on butene uptake, but a negative effect on isobutane uptake, which suggests that PLD is probably an important factor to adjust the adsorption selectivity of isobutane to butene for zeolite-catalyzed alkylation. The influence of structures on the butene uptake is greater than that of isobutane when the feed of I/O is 1:1 and decreases with increasing the I/O feed ratio. Moreover, the huge difference for the effect of LCD on isobutane and butene amount implies that LCD may play an important role in the adsorption behaviors.

As for thermal properties, there is a positive effect of  $Q_{st}$  of butene ( $Q_{st}, C4=$ ) on uptakes of butene; that is, the higher  $Q_{st}, C4=$  corresponds to a higher adsorption ability of butene. In fact, as the I/O feed ratio increases, the amount of adsorbed butene decreases and the influence of  $Q_{st}, C4=$  increases, indicating that the interaction between the unsaturated butene and the zeolite framework is prior. However, the

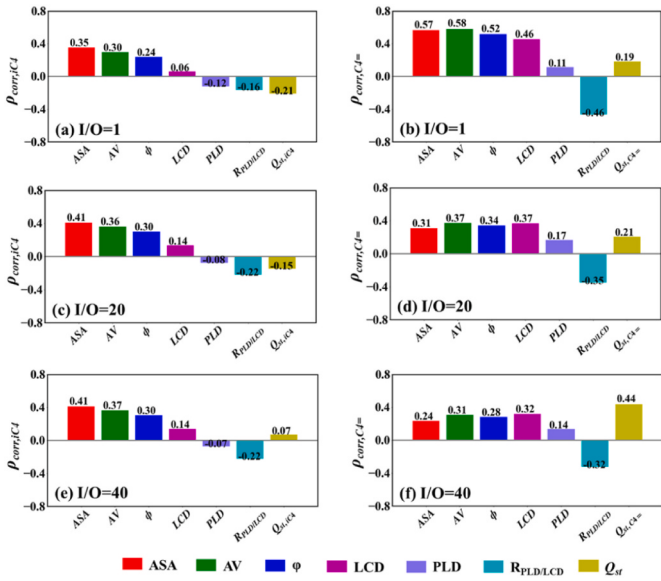


**Fig. 2.** Pearson correlation coefficients of the adsorption uptakes of isobutane and butene with structural features of zeolites and thermal parameters. (a), (c), and (e) represent the correlation for isobutane. (b), (d), and (f) represent the correlation for butene.  $Q_{st, iC4}$  and  $Q_{st, C4}$  represent the isosteric adsorption heat of isobutane and 1-butene, respectively.

correlation of the adsorption heat ( $Q_{st, iC4}$ ) and the uptake for isobutane shows the different results. The  $Q_{st, iC4}$  has a negative correlation with isobutane adsorption capacity at the feed I/O ratio of 1:1 and 20:1, which indicates that the interaction between isobutane and zeolite framework plays a leading role. When the feed I/O ratio reaches 40:1, the negative correlation of isobutane adsorption heat on the adsorption of isobutane turns into a positive effect. This is probably because excessive isobutane molecules fill up the pores of the zeolite, reducing the distance between isobutane molecules and thereby increasing the interaction force between isobutane molecules.

To increase the alkylation conversion rate and extend the lifetime of the catalyst, increasing the adsorption capacity of C4 reactants on the zeolites as much as possible and the adsorption selectivity of isobutane to butene is the optimal choice. As indicated in Fig. 2, all the parameters with high values benefit to the adsorption amount of C4 reactants, except the PLD,  $R_{PLD}/LCD$ , and  $Q_{st}$ . The influence of LCD is significantly different in the adsorption capacity of butene and isobutane. In addition, the  $R_{PLD}/LCD$  consists of PLD and LCD. Thus, the PLD, LCD, and  $Q_{st}$  are considered as key parameters to discuss adsorption selectivity. The relationships between the three parameters and the selectivity of isobutane to butene ( $S_{iC4/C4^=}$ ) were plotted in Fig. 3. As shown in Fig. 3, a higher selectivity of isobutane to butene ( $S_{iC4/C4^=}$ ) is observed with low  $Q_{st, iC4}$  at every feed I/O ratio. Meanwhile,  $S_{iC4/C4^=}$  drops with increasing LCD, suggesting that the zeolite with the large LCD is not preferential for selective adsorption of isobutane. Indeed, the highest  $S_{iC4/C4^=}$  is approximately ten at a small LCD, which is comparable with the diameter of isobutane. The PLD shows the similar effect on  $S_{iC4/C4^=}$ . Furthermore, a slight increase in the heat of adsorption can be observed as the feed I/O ratio increases when the LCD or PLD is in the range of 5–10 Å, suggesting that the adsorption of iC4 is more favorable in confined spaces. There is also no obvious influence of feed I/O ratio on the correlation between the adsorption characteristics of C4 reactants and the structural features of zeolites. A similar phenomenon of  $Q_{st, C4^=}$  on  $S_{iC4/C4^=}$  also exists in the competitive adsorption of C4 reactants system (see Fig. S4). Nonetheless, the difference is not significant compared to the effect of the heat of adsorption on the selectivity of isobutane to butene, which means that the zeolite pore size is the most critical factor affecting the adsorption behavior of C4 reactants.

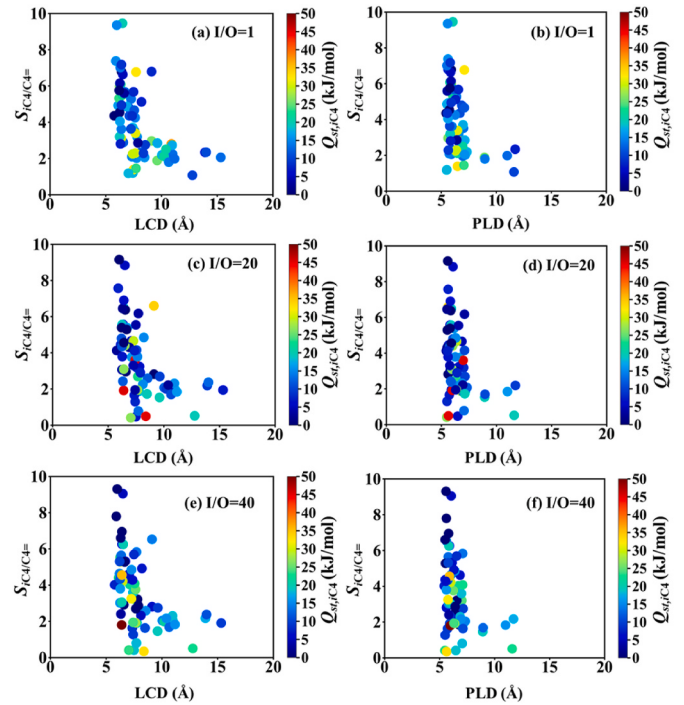


**Fig. 3.** The structure-performance relationship of selectivity of isobutane to butene and three physical-chemical parameters in selected zeolites at three feed ratios.  $Q_{st, iC4}$  represents the isosteric adsorption heat of isobutane.

### 3.2. Diffusion characteristics

The diffusion coefficient ( $D$ ), especially of isobutane, in the micro-pore of zeolites, is also another important dynamic factor to determine the alkylate distributions and the lifetime of zeolite catalysts for solid acid alkylation. Thus, the  $D$  of isobutane and butene in the micropore of all the pre-screened 70 zeolites were obtained using MD simulations with the initial structures taken from the equilibrated configurations of CBMC runs. The results are included in Table S4. To correlate the dynamics property of C4 reactants and structural features of zeolites, the  $\rho_{corr}$  of the  $D$  of isobutane and butene with the structure parameters zeolite were obtained, as shown in Fig. 4. Obviously, the effect of the structure parameters of zeolites on  $D$  of C4 reactants and the effect of zeolite structure parameters on adsorption of C4 reactants showed relatively opposite trends. The correlation of the diffusion behavior is opposite to that of the adsorption behavior, but the parameters with the most significant effect are the same, namely LCD and PLD. The highest correlation coefficient between  $R_{PLD}/LCD$  and PLD and diffusion indicates that the influence of channel structure on the diffusion of C4 reactants is obvious [27]. It also can be observed that the degree of negative correlation of ASA, AV, and  $\varphi$  to the isobutane diffusion coefficient increases with the feed I/O ratio. However, with the increase of the proportion of raw olefins, ASA has little effect on the butene diffusion coefficient, while the effect of volume and porosity on the butene diffusion coefficient is slightly larger. The different phenomena regarding the correlation coefficients of isobutane and butene with ASA, AV, and  $\varphi$  can be attributed to the fact that more isobutane occupancy within the zeolite pores makes less space available for molecular movement. Furthermore, the increase in the number of C4 reactants enhances the free energy barrier of molecules to move, similar to methane diffusion in zeolites [59]. Considering that ASA, AV, and  $\varphi$  of zeolite are directly related to the channel structure, and PLD, LCD and  $R_{PLD}/LCD$  can represent the channel structure of the zeolite, it can be concluded that the diffusion of C4 reactants depends on the PLD, LCD and  $R_{PLD}/LCD$  of zeolite.

Since the acidic active sites of zeolite have a strong self-aggregation

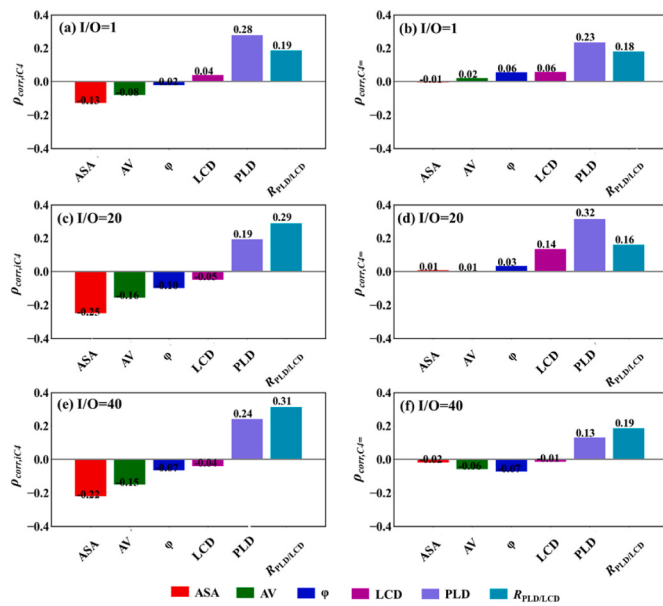


**Fig. 4.** Pearson correlation coefficients of the self-diffusion of isobutane and butene with structural features of zeolites. (a), (c), and (e) represent the correlation for the self-diffusion of isobutane. (b), (d), and (f) represent the correlation for the self-diffusion of butene.

tendency and butene oligomerization activity, the fast diffusion rate of butene can promote the self-aggregation phenomenon and further enhance the oligomerization of butene in the microenvironment around active sites. Given that the pore structure influences the molecule diffusion, the higher  $D$  of isobutane is required to competitively occupy the reactive sites to inhibit the oligomerization of butene.  $D_{iC4/C4^-}$  is also an important parameter to influence the lifetime of zeolite catalysts. Thus, Fig. 5 displayed the structure-performance relationship of  $D_{iC4/C4^-}$  with PLD, LCD, and  $R_{PLD/LCD}$  in selected zeolites at three feed ratios. As

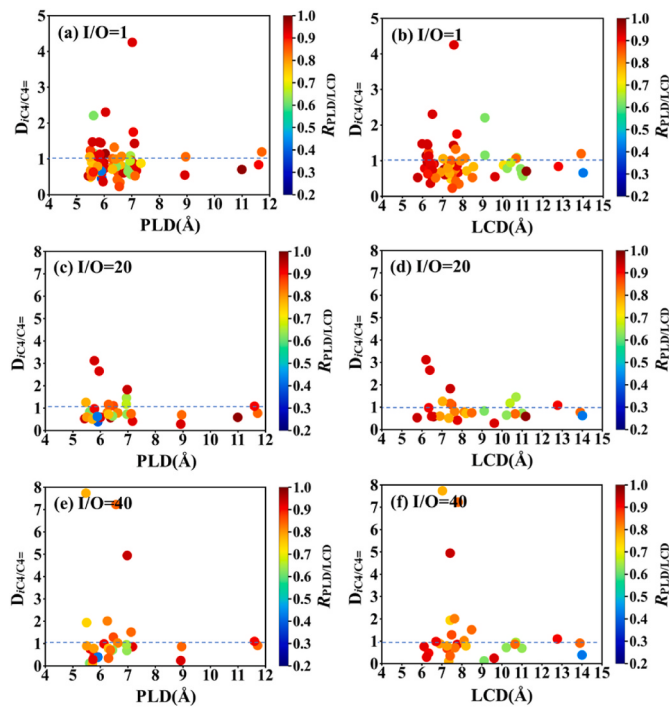


**Fig. 5.** The structure-performance relationship of relative diffusion coefficients with PLD, LCD, and  $R_{PLD/LCD}$  in selected zeolites at three feed ratios.

illustrated in Fig. 5, most zeolites have a pore size in the range of 5.5 and 8 Å. The best  $D_{iC4/C4^-}$  exists at both PLD and LCD close to 7 Å. With the increase in feed ratios, the number of zeolites with  $D_{iC4/C4^-} > 1$  and LCD > 9 Å changes a little. When the  $D_{iC4/C4^-} > 1$ , the  $R_{PLD/LCD}$  is higher than 0.6, and the  $R_{PLD/LCD}$  of the best  $D_{iC4/C4^-}$  is approximately 1, which suggests the confinement effect of zeolite pores. Combined with the effect of pore confinement on the diffusion and adsorption selectivity of the C4 reactants, it can be predicted that the pore structure of the zeolite will greatly affect the adsorption and diffusion of the C4 reactants, thereby affecting the alkylation reaction.

### 3.3. Relationships of adsorption and diffusion

As described in the previous sections, the high adsorption selectivity and the relative diffusion coefficient of isobutane to butene are greatly important for C4 alkylation using zeolite catalysts. The specific adsorption selectivity of isobutane to butene ( $S_{iC4/C4^-}$ ) of the zeolite frameworks that can simultaneously adsorb isobutane and 1-butene at the three feed ratios are listed in Table S5. Since the change of the feed ratio has little effect on the  $S_{iC4/C4^-}$ , the  $S_{iC4/C4^-}$  and the relative diffusion coefficient ( $D_{iC4/C4^-}$ ) of isobutane to butene were correlated with the feed ratio of 1, as shown in Fig. 6. The zeolites can be divided into three groups, including top suitable zeolites (crimson pentagram) with  $D_{iC4/C4^-} > 1$ , second suitable zeolites (blue pentagram) with  $S_{iC4/C4^-} > 3$ , and the third suitable zeolites (green pentagram) with  $S_{iC4/C4^-} < 3$  and  $D_{iC4/C4^-} < 1$ . Theoretically, top suitable zeolites with high  $S_{iC4/C4^-}$  and  $D_{iC4/C4^-}$  are conducive to alkylation reaction, but adsorption capacity and practical diffusion rate also affect the alkylation reaction. Therefore, 12 zeolites with  $D_{iC4/C4^-} > 1$  or  $S_{iC4/C4^-} > 3$  are selected to further discuss the influence on adsorption and diffusion behaviors, as listed in Table 1.

According to Table 1, the  $S_{iC4/C4^-}$  in AFR, IFO, ISV, IWS, IWR, and SAO topologies is higher than 3, and the  $D_{iC4/C4^-}$  of FAU, IRR, IRY, IWV, SFN, and SFS topologies is greater than or equal to 1. As described in Table 1, it can be found that the dimension of channels influences the total uptake of C4, where the 3D channels with higher ASA have larger adsorption uptake compared to the two-dimensional (2D) or 1D channels, but has no obvious effects on the adsorption selectivity and relative diffusion. Whereas, the zeolite topologies with  $S_{iC4/C4^-} > 4$  have 3D channels. Furthermore, the zeolites can be divided into three groups, the first group is FAU, IRR, and IRY. The second group is 3D zeolites with the highest  $S_{iC4/C4^-}$  including ISV, IWR, IWS, and SAO. The remaining 1D or

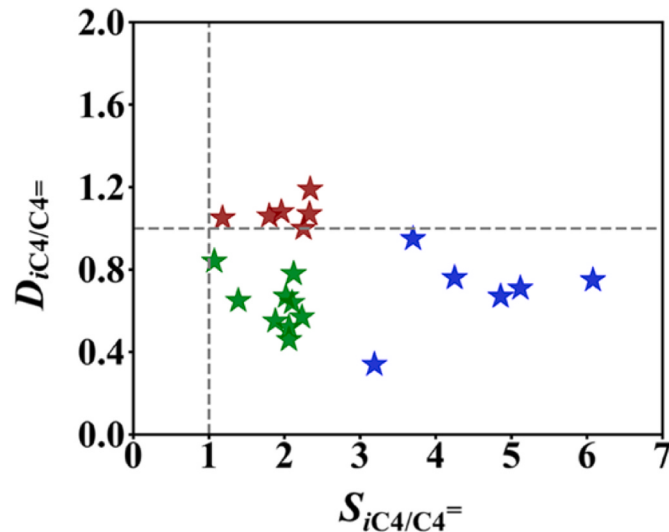


**Fig. 6.** Structure-performance relationship between the adsorption selectivity and relative diffusion coefficient of isobutane to butene and the  $R_{PLD/LCD}$ , ASA, LCD, and PLD of zeolites at feed I/O = 1.

**Table 1**Zeolites with  $D_{IC4/C4^+} \geq 1$  or  $S_{IC4/C4^+} > 3$ .

Group	Topology	Channel dimension	Limiting ring <sup>a</sup>	ASA ( $\text{m}^2/\text{g}$ )	PLD ( $\text{\AA}$ )	LCD ( $\text{\AA}$ )	$R_{\text{PLD}}/\text{LCD}$	$N_{\text{total},1}$	$S_{IC4/C4}^-$	$D_{IC4/C4}^-$
1	FAU	3	12	968.1	7.0	10.7	0.6	255	2.0	1.1
	IRR	3	18/12	856.6	11.7	13.9	0.8	101	2.3	1.2
	IRY	3	16/15	1088.5	9.0	10.7	0.8	85	1.8	1.1
2	ISV	3	12	876.2	5.8	6.3	0.9	166	6.1	0.8
	SAO	3	12	1040.7	6.3	8.2	0.8	170	5.1	0.7
	IWR	3	12/10	766.4	5.5	6.9	0.8	143	4.9	0.7
3	IWS	3	12/12	912.4	6.3	7.6	0.8	237	4.3	0.8
	IFO	1	16	546.5	7.0	7.4	0.9	74	3.7	0.9
	SFN	1	14	524.2	6.3	7.4	0.8	69	2.2	1.0
	AFR	2	12/8	704.1	6.6	7.8	0.8	65	3.2	0.3
	IWV	2	12	796.4	6.6	8.1	0.8	75	2.3	1.1
	SFS	2	12/10	626.1	5.5	7.0	0.8	77	1.2	1.1

<sup>a</sup> The limiting ring size of the apertures of zeolite frameworks, which usually interprets the kinetic accessibility and catalytic test reaction in a given material [60].

2D zeolites with the lowest total uptake containing AFR, IWV, SFS, IFO, and SFN are the third group. The structure snaps are shown in Fig. S5.

### 3.4. Optimal zeolites

FAU, ISV, IFO, AFR were selected as the typical frameworks to further explore the influence of topologies on the adsorption and diffusion performances by calculating the number densities of C4 reactants at I/O = 1 in xy and yz planes, the results were shown in Fig. 7. As plotted in Fig. 7, the distribution of C4 reactants in FAU is the most uniform in the xy and yz planes. The number density of C4 molecules in the other three zeolite topologies is at least 1.5 times than that in FAU. Furthermore, the number density of isobutane in 2D IFO topology on the xy plane is about ten times than that in FAU topology. By comparing the number density distribution of C4 reactants in the FAU and ISV

topologies, the ISV topology with narrow cross-shaped pores have higher isobutane selectivity, but the narrow and long channels inhibit relative diffusion of isobutane. Furthermore, to the best of our knowledge, the presence of germanium element in acidic ISV zeolite may suffer from low hydrothermal stability [61,62], which is not conducive to the long-term use of zeolite in alkylation reactions. As for FAU-type zeolites, the unique super-cage of FAU-type generates a unique confinement combined with spatial constraint and electric field, making the catalytic activity. Aluminosilicate FAU-type zeolites, including X and Y zeolites, have been widely used to study the isobutane alkylation process [63,64].

Although the selectivity and relative diffusion coefficient of isobutane in 1D and 2D straight pores are similar to those in 3D large pores, the total adsorption capacity is quite small, which can be attributed to the spatial constraint in the channels. From Fig. 7c, it is clear that the

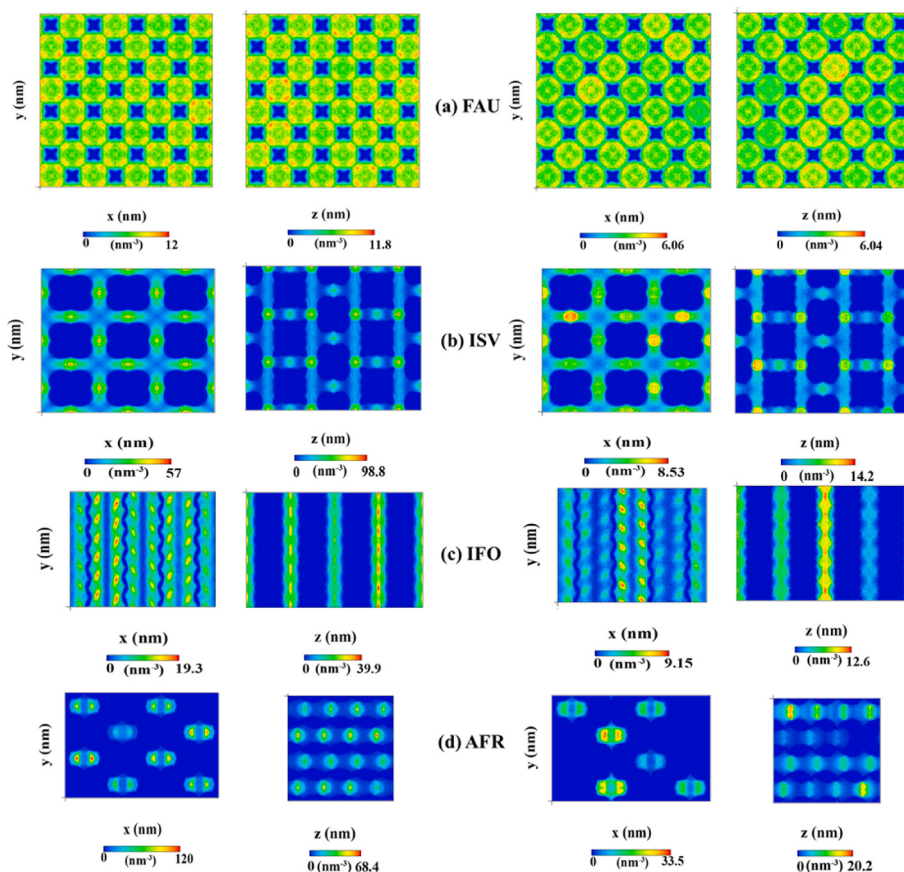


**Fig. 7.** Densities of C4 molecules at I/O = 1 (feed ratio) in (a) FAU, (b) ISV, (c) IFO, (d) AFR in xy and yz planes.

smaller gap between the channel junction and the channel size leads to a better distribution of C4 reactants, which is conducive to the diffusion of C4 reactants. The abnormal diffusion of 2D AFR may be attributed to the narrow intersections for the two channels. IFO-type and AFR-type zeolites usually occur in the form of silicoaluminophosphate, which generally can be classified as mildly acidic catalysts [65]. Given that the isobutane alkylation reaction is performed with the strong acid, the acidity of silicoaluminophosphate should be increased. In addition, the high hydrophilic surface properties of silicoaluminophosphate may promote the accumulation of butene and result in oligomerization of butene [65]. However, both IFO and AFR materials have large pore size, especially IFO-type with 16-ring extra-large pore size [66,67]. The large channels (IFO) are benefit to the diffusion of the alkylation products and inhibit the side reactions. It is possible to catalyze the isobutane alkylation by enhancing the acidity strength of silicoaluminophosphate and decreasing the hydrophilic ability of silicoaluminophosphate zeolite.

### 3.5. Interactions between C4 reactants and zeolites

The effect of the topology on the adsorption and diffusion behaviors of alkylation reactants was further clarified by the comparison of center-of-mass radial distribution function (RDF) of isobutane and butene in the zeolite pores, which are shown in Fig. 8 a-c and Fig. S6. As demonstrated in Fig. S6, the RDF of isobutane and O atom on the zeolite ( $i\text{C}4-\text{O}(\text{SiO}_2)$ ) is very similar to the RDF of butene and O atom on the same zeolite ( $\text{C}4^=\text{-O}(\text{SiO}_2)$ ), implying the all-silica zeolites without acid sites have the similar attraction to isobutane and butene. It can be seen from Fig. 8a and b that different pore structures have different interactions for isobutane and butene. Due to the similar size of the isobutane kinetic diameter and the limiting ring of channels in zeolites, including ISV with 3D straight cross channels and AFR with 2D gourd-shaped channels, the diffusion of C4 reactants, especially isobutane, is limited. Moreover, the distance between the zeolite (ISV/AFR) and C4 molecules is smaller than that between FAU with 3D connected large channels or IFO with 1D straight large channels, indicating a stronger interaction of C4 molecules and ISV or AFR than that and FAU or IFO. On the contrary, the center-of-mass RDF of isobutane and butene in zeolites shows the opposite

results (see Fig. 8c), suggesting that the weak interaction of guest-framework and the strong interaction of isobutane/butene benefit the reduction of intermolecular distance for the C4 reactants and the increase in the probability of alkylation reaction. Furthermore, Fig. 8d shows the center of mass Lennard-Jones (LJ) potential surface of isobutane and butene molecules in the zeolite pores. As demonstrated in Fig. 8d, the van der Waals interaction of guest-framework and isobutane/butene decreases with the increase of the distance. When the distance is greater than 3.8 Å, there is a little difference between  $i\text{C}4-\text{O}(\text{SiO}_2)$  and  $\text{C}4^=\text{-O}(\text{SiO}_2)$  in the van der Waals force level. The same phenomenon exists between  $i\text{C}4-\text{C}4^=$  and  $\text{C}4^=\text{-O}(\text{SiO}_2)$ , when the distance is greater than 4.5 Å. Considering the similar pore size of selected zeolites and isobutane kinetic diameter, the distance between the center-of-mass of isobutane/1-butene and O atom from the zeolite can be guaranteed to be higher than 3.8 Å, but the pore size of zeolites cannot satisfy the distance between isobutane center-of-mass and butene center-of-mass higher than 4.5 Å, which corroborates the results shown in Fig. 8a-c and leads to the accumulation of both isobutane and butene at the connection of channels.

### 4. Conclusions

The adsorption and diffusion properties of C4 reactants in 70 all-silica zeolites for solid acid alkylation were calculated using CBMC and MD simulations to establish the structure-performance relationship. The adsorption capacity and diffusion coefficient of isobutane/butene were correlated with physical-thermal properties of zeolites to obtain the most relevant parameters. The bulk composition change of C4 reactants has little influence on the adsorption selectivity of isobutane. The pore structures including PLD, LCD,  $R_{\text{PLD}}/\text{LCD}$ , and the channel dimension are the most relevant parameters.

Zeolites with 3D connected channels and large LCD, ASA such as FAU have high C4 adsorption uptake, moderate selectivity, and relative diffusion coefficient, which may be the suitable topologies. High interaction of C4 reactants lead to the lower self-diffusion coefficient than the general diffusion coefficient in 1D straight channels. The narrow connection of channels in some zeolites with 2D channels seriously

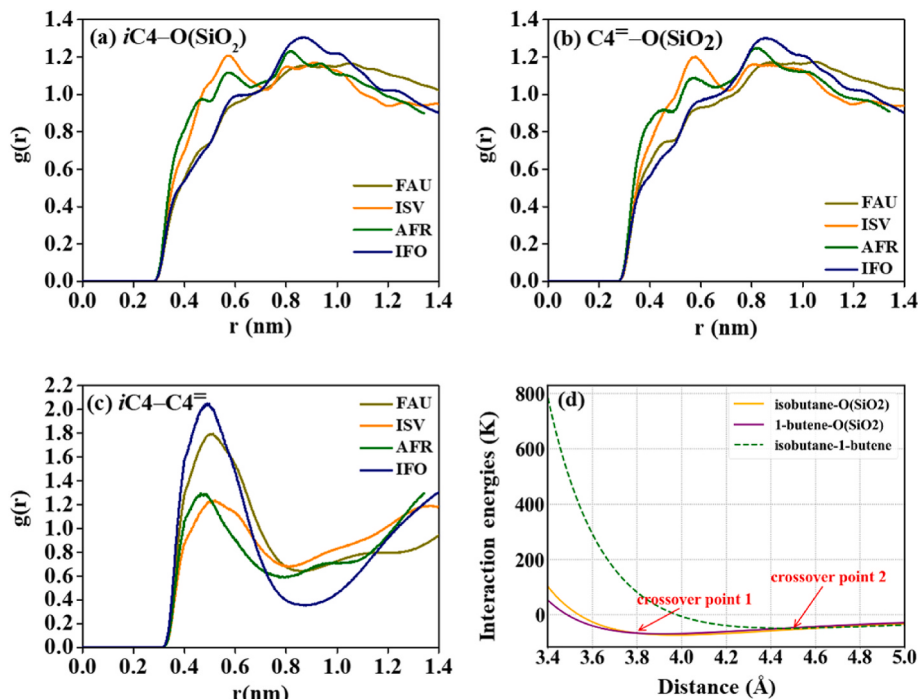


**Fig. 8.** (a–c) Center-of-mass RDF of isobutane and 1-butene molecules in the zeolite pores. (d) Center-of-mass Lennard-Jones (L–J) potential surface of isobutane and 1-butene molecules in the zeolite pores.

inhibits the diffusion of isobutane molecules. The mild acidic silicoaluminophosphate with large pore size makes it possible to promote the diffusion of product inhibit the deactivation of catalysts.

### CRediT authorship contribution statement

**Bihong Li:** Writing – original draft, Validation, Software, Methodology, Data curation. **Pan Huang:** Software, Methodology, Data curation, Conceptualization. **Piao Cao:** Data curation. **Weiqun Gao:** Data curation. **Weizhong Zheng:** Writing – review & editing, Visualization, Methodology, Conceptualization. **Cheng Lian:** Supervision, Methodology, Conceptualization. **Weizhen Sun:** Writing – review & editing, Supervision, Project administration, Funding acquisition. **Ling Zhao:** Supervision, Project administration.

### Declaration of competing interest

The authors declare that they have no known competing financial interests or personal relationships that could have appeared to influence the work reported in this paper.

### Acknowledgments

Financial support by the National Natural Science Foundation of China (91434108) is gratefully acknowledged.

### Appendix A. Supplementary data

Supplementary data to this article can be found online at <https://doi.org/10.1016/j.micromeso.2022.112040>.

### References

- [1] M.A. Fahim, T.A. Alsahaf, A. Elkilani, Chapter 10 - alkylation, in: M.A. Fahim, T. A. Alsahaf, A. Elkilani (Eds.), Fundamentals of Petroleum Refining, Elsevier, Amsterdam, 2010, pp. 263–283.
- [2] D.A. Nafis, K.A. Detrick, R.L. Mehlberg, Alkylation in petroleum processing, in: S. A. Treese, D.S. Jones, P.R. Pujado (Eds.), Handbook of Petroleum Processing, Springer International Publishing, Cham, 2015, pp. 1–17.
- [3] Y. Li, R. Liu, G. Zhao, Z. Zhou, J. Zhang, C. Shi, X. Liu, X. Zhang, S. Zhang, Simulation and optimization of fixed bed solid acid catalyzed isobutane/2-butene alkylation process, *Fuel* 216 (2018) 686–696.
- [4] Y. Liu, G. Liu, G. Wu, R. Hu, Alkylation of isobutane and 2-butene in rotating packed-bed reactors: using ionic liquid and solid acid as catalysts, *Ind. Eng. Chem. Res.* 59 (2020) 14767–14775.
- [5] S. Singhal, S. Agarwal, S. Arora, N. Singhal, A. Kumar, Solid acids: potential catalysts for alkene-isoalkane alkylation, *Catal. Sci. Technol.* 7 (2017) 5810–5819.
- [6] B.O. Dalla Costa, C.A. Querini, Isobutane alkylation with butenes in gas phase, *Chem. Eng. J.* 162 (2010) 829–835.
- [7] K. Yoo, E.C. Burckle, P.G. Smirniotis, Isobutane/2-Butene alkylation using large-pore zeolites: influence of pore structure on activity and selectivity, *J. Catal.* 211 (2002) 6–18.
- [8] J. Liu, N. Ding, X. Hong, S. Zhou, X. Zhou, J.A. Wang, L. Chen, Isobutane/1-butene alkylation performance of ammonium fluoride-modified HUSY zeolite, *Catal. Lett.* 150 (2020) 2996–3006.
- [9] S. Sahebdelfar, M. Kazemeini, F. Khorasheh, A. Badakhshan, Deactivation behavior of the catalyst in solid acid catalyzed alkylation: effect of pore mouth plugging, *Chem. Eng. Sci.* 57 (2002) 3611–3620.
- [10] C.A. Querini, E. Roa, Deactivation of solid acid catalysts during isobutane alkylation with C4 olefins, *Appl. Catal. Gen.* 163 (1997) 199–215.
- [11] A. Feller, J.-O. Barth, A. Guzman, I. Zuazo, J.A. Lercher, Deactivation pathways in zeolite-catalyzed isobutane/butene alkylation, *J. Catal.* 220 (2003) 192–206.
- [12] S. Ramachandran, T.G. Lenz, W.M. Skiff, A.K. Rappé, Toward an understanding of zeolite Y as a cracking catalyst with the use of periodic charge equilibration, *J. Phys. Chem.* 100 (1996) 5898–5907.
- [13] C. Liu, R.A. van Santen, A. Pouraeidesfahani, T.J.H. Vlugt, E.A. Pidko, E.J. M. Hensen, Hydride transfer versus deprotonation kinetics in the isobutane-propene alkylation reaction: a computational study, *ACS Catal.* 7 (2017) 8613–8627.
- [14] H. Díaz Velázquez, N. Likhanova, N. Aljammal, F. Verpoort, R. Martínez-Palou, New insights into the progress on the isobutane/butene alkylation reaction and related processes for high-quality fuel production. A critical review, *Energy Fuel.* 34 (2020) 15525–15556.
- [15] J.M. Martinis, G.F. Froment, Alkylation on solid acids. Part 1. Experimental investigation of catalyst deactivation, *Ind. Eng. Chem. Res.* 45 (2006) 940–953.
- [16] S.O. Omarov, E.A. Vlasov, D.A. Sladkovskiy, K.V. Semikin, A.N. Matveyeva, S. P. Fedorov, G.V. Oganesyan, D.Y. Murzin, Physico-chemical properties of  $\text{MoO}_3/\text{ZrO}_2$  catalysts prepared by dry mixing for isobutane alkylation and butene transformations, *Appl. Catal. B Environ.* 230 (2018) 246–259.
- [17] A. Feller, I. Zuazo, A. Guzman, J.O. Barth, J.A. Lercher, Common mechanistic aspects of liquid and solid acid catalyzed alkylation of isobutane with n-butene, *J. Catal.* 216 (2003) 313–323.
- [18] F. Schüller, S. Schallmoser, H. Shi, G.L. Haller, E. Ember, J.A. Lercher, Enhancement of dehydrogenation and hydride transfer by  $\text{La}^{3+}$  cations in zeolites during acid catalyzed alkane reactions, *ACS Catal.* 4 (2014) 1743–1752.
- [19] H. Zhang, J. Xu, H. Tang, Z. Yang, R. Liu, S. Zhang, Isobutane/2-Butene alkylation reaction catalyzed by Cu-modified and rare earth X-type zeolite, *Ind. Eng. Chem. Res.* 58 (2019) 9690–9700.
- [20] A. Corma, V. Gómez, A. Martínez, Zeolite beta as a catalyst for alkylation of isobutane with 2-butene. Influence of synthesis conditions and process variables, *Appl. Catal. Gen.* 119 (1994) 83–96.
- [21] M.F. Simpson, J. Wei, S. Sundaresan, Kinetic analysis of isobutane/butene alkylation over ultrastable H-Y zeolite, *Ind. Eng. Chem. Res.* 35 (1996) 3861–3873.
- [22] D.A. Sladkovskiy, K.V. Semikin, A.V. Utemov, S.P. Fedorov, E.V. Sladkovskaya, N. V. Kuzichkin, A. Aho, D.Y. Murzin, Comparison of isobutane/n-butenes alkylation over Y-zeolite catalyst in CSTR, fixed bed and circulating flow reactors, *Rev. J. Chem.* 10 (2020) 58–72.
- [23] Y.F. Chu, A.W. Chester, Reactions of isobutane with butene over zeolite catalysts, *Zeolites* 6 (1986) 195–200.
- [24] A.L. Mota Salinas, G. Sapaly, Y. Ben Taarit, J.C. Vedrine, N. Essayem, Continuous supercritical iC4/C4= alkylation over H-Beta and H-USY Influence of the zeolite structure, *Appl. Catal. Gen.* 336 (2008) 61–71.
- [25] A. Corma, A. Martínez, Chemistry, catalysts, and processes for isoparaffin-olefin alkylation: actual situation and future trends, *Catal. Rev.* 35 (1993) 483–570.
- [26] A. Luna-Triguero, A. Slawek, R. Sánchez-de-Armas, J.J. Gutiérrez-Sevillano, C. O. Ania, J.B. Parra, J.M. Vicent-Luna, S. Calero,  $\pi$ -Complexation for olefin/paraffin separation using aluminosilicates, *Chem. Eng. J.* 380 (2020), 122482.
- [27] Z. Liu, J. Zhou, X. Tang, F. Liu, J. Yuan, G. Li, L. Huang, R. Krishna, K. Huang, A. Zheng, Dependence of zeolite topology on alkane diffusion inside diverse channels, *AIChE J.* 66 (2020), e16269.
- [28] B. Smit, Molecular simulations of zeolites: adsorption, diffusion, and shape selectivity, *Chem. Rev.* 108 (2008) 4125–4184.
- [29] Y. Zhang, J. Xu, X. Tang, C. Yang, Simulation study on adsorption and diffusion properties of alkylation reaction components in hierarchical zeolites, *Comput. Appl. Chem.* 36 (2019) 659–663.
- [30] P. Cao, B. Li, W. Sun, L. Zhao, Understanding the zeolites catalyzed isobutane alkylation based on their topology effects on the reactants adsorption, *Chem. Eng. Sci.* 250 (2022), 117387.
- [31] C. Baerlocher, L.B. McCusker, Database of zeolite structures. <http://www.iza-structure.org/databases/>. Last accessed 2021.
- [32] T.F. Willems, C.H. Rycroft, M. Kazi, J.C. Meza, M. Haranczyk, Algorithms and tools for high-throughput geometry-based analysis of crystalline porous materials, *Microporous Mesoporous Mater.* 149 (2012) 134–141.
- [33] P. Gómez-Álvarez, A.R. Ruiz-Salvador, S. Hamad, S. Calero, Importance of blocking inaccessible voids on modeling zeolite adsorption: revisited, *J. Phys. Chem. C* 121 (2017) 4462–4470.
- [34] B. Widom, Some topics in the theory of fluids, *J. Chem. Phys.* 39 (1963) 2808–2812.
- [35] Y. Zhang, J. Xu, X. Tang, C. Yang, Simulation of multi-component adsorption and deactivation mechanism of alkylation reaction in zeolites, *Acta Pet. Sin.* 36 (2020) 86–94.
- [36] J.-P. Ryckaert, A. Bellemans, Molecular dynamics of liquid alkanes, *Faraday Discuss. Chem. Soc.* 66 (1978) 95–106.
- [37] P. Cao, W. Zheng, W. Sun, L. Zhao, The shape selectivity of zeolites in isobutane alkylation: an investigation using CBMC and MD simulations, *Chem. Eng. Sci.* 245 (2021), 116966.
- [38] D. Dubbeldam, S. Calero, T.J.H. Vlugt, R. Krishna, T.L.M. Maesen, B. Smit, United atom force field for alkanes in nanoporous materials, *J. Phys. Chem. B* 108 (2004) 12301–12313.
- [39] M.A. Granato, N. Lamia, T.J. Vlugt, A.E. Rodrigues, Adsorption equilibrium of isobutane and 1-butene in zeolite 13X by molecular simulation, *Ind. Eng. Chem. Res.* 47 (2008) 6166–6174.
- [40] B. Liu, B. Smit, S. Calero, Evaluation of a new force field for describing the adsorption behavior of alkanes in various pure silica zeolites, *J. Phys. Chem. B* 110 (2006) 20166–20171.
- [41] S. Calero, D. Dubbeldam, R. Krishna, B. Smit, T.J.H. Vlugt, J.F.M. Denayer, J. A. Martens, T.L.M. Maesen, Understanding the role of sodium during adsorption: a force field for alkanes in sodium-exchanged faujasites, *J. Am. Chem. Soc.* 126 (2004) 11377–11386.
- [42] A.G. Bezus, A.V. Kiselev, A.A. Lopatkin, P.Q. Du, Molecular statistical calculation of the thermodynamic adsorption characteristics of zeolites using the atom–atom approximation. Part 1.—adsorption of methane by zeolite  $\text{NaX}$ , *J. Chem. Soc., Faraday Trans. 2: Mol. Chem. Phys.* 74 (1978) 367–379.
- [43] P. Huang, Z. Yin, Y. Tian, J. Yang, W. Zhong, C. Li, C. Lian, L. Yang, H. Liu, Anomalous diffusion in zeolites, *Chem. Eng. Sci.* 246 (2021), 116995.
- [44] J. Kuhn, J.M. Castillo-Sánchez, J. Gascon, S. Calero, D. Dubbeldam, T.J.H. Vlugt, F. Kapteijn, J. Gross, Adsorption and diffusion of water, methanol, and ethanol in all-silica DD3R: experiments and simulation, *J. Phys. Chem. C* 113 (2009) 14290–14301.

- [45] D. Frenkel, B. Smit, Monte Carlo simulations in various ensembles, in: D. Frenkel, B. Smit (Eds.), Understanding Molecular Simulation: from Algorithms to Applications, Elsevier, Amsterdam, 2001, pp. 109–135.
- [46] J.I. Siepmann, D. Frenkel, Configurational bias Monte Carlo: a new sampling scheme for flexible chains, *Mol. Phys.* 75 (1992) 59–70.
- [47] S. Jakobtorweihen, N. Hansen, F.J. Keil, Molecular simulation of alkene adsorption in zeolites, *Mol. Phys.* 103 (2005) 471–489.
- [48] R.W. Hockney, S.P. Goel, J.W. Eastwood, Quiet high-resolution computer models of a plasma, *J. Comput. Phys.* 14 (1974) 148–158.
- [49] W.G. Hoover, Canonical dynamics: equilibrium phase-space distributions, *Phys. Rev. A* 31 (1985) 1695.
- [50] S. Nosé, A molecular dynamics method for simulations in the canonical ensemble, *Mol. Phys.* 52 (1984) 255–268.
- [51] D. Dubbeldam, S. Calero, D.E. Ellis, R.Q. Snurr, RASPA: molecular simulation software for adsorption and diffusion in flexible nanoporous materials, *Mol. Simulat.* 42 (2016) 81–101.
- [52] D. Van Der Spoel, E. Lindahl, B. Hess, G. Groenhof, A.E. Mark, H.J.C. Berendsen, GROMACS: fast, flexible, and free, *J. Comput. Chem.* 26 (2005) 1701–1718.
- [53] S. Amirjalayer, M. Tafipolsky, R. Schmid, Molecular dynamics simulation of benzene diffusion in MOF-5: importance of lattice dynamics, *Angew. Chem. Int. Ed.* 46 (2007) 463–466.
- [54] T. Méndez-Morales, J. Carrete, M. García, O. Cabeza, L.J. Gallego, L.M. Varela, Dynamical properties of alcohol + 1-Hexyl-3-methylimidazolium ionic liquid mixtures: a computer simulation study, *J. Phys. Chem. B* 115 (2011) 15313–15322.
- [55] R. Chitra, S. Yashonath, Estimation of error in the diffusion coefficient from molecular dynamics simulations, *J. Phys. Chem. B* 101 (1997) 5437–5445.
- [56] L.N. Gergidis, D.N. Theodorou, Molecular dynamics simulation of n-Butane–Methane mixtures in silicalite, *J. Phys. Chem. B* 103 (1999) 3380–3390.
- [57] B.C. Yeo, D. Kim, H. Kim, S.S. Han, High-throughput screening to investigate the relationship between the selectivity and working capacity of porous materials for propylene/propane adsorptive separation, *J. Phys. Chem. C* 120 (2016) 24224–24230.
- [58] A. Feller, J.A. Lercher, Chemistry and technology of isobutane/alkene alkylation catalyzed by liquid and solid acids, *Adv. Catal.* 48 (2004) 229–225.
- [59] E. Beerdsen, D. Dubbeldam, B. Smit, Loading dependence of the diffusion coefficient of methane in nanoporous materials, *J. Phys. Chem. B* 110 (2006) 22754–22772.
- [60] X. Li, M.W. Deem, Why zeolites have so few seven-membered rings, *J. Phys. Chem. C* 118 (2014) 15835–15839.
- [61] M.V. Shamzhy, P. Eliašová, D. Vitvarová, M.V. Opanasenko, D.S. Firth, R.E. Morris, Post-Synthesis stabilization of germanosilicate zeolites ITH, IWW, and UTL by substitution of Ge for Al, *Chem. A Eur. J.* 22 (2016) 17377–17386.
- [62] S. Leiva, M.J. Sabater, S. Valencia, G. Sastre, V. Fornés, F. Rey, A. Corma, A new synthesis method for the preparation of ITQ-7 zeolites and the characterisation of the resulting materials, *Compt. Rendus Chem.* 8 (2005) 369–378.
- [63] A. Feller, A. Guzman, I. Zuazo, J.A. Lercher, On the mechanism of catalyzed isobutane/butene alkylation by zeolites, *J. Catal.* 224 (2004) 80–93.
- [64] E.R. Naranov, K.I. Dement'ev, I.M. Gerzeliev, N.V. Kolesnichenko, E.A. Roldugina, A.L. Maksimov, The role of zeolite catalysis in modern petroleum refining: contribution from domestic technologies, *Petrol. Chem.* 59 (2019) 247–261.
- [65] B.M. Lok, C.A. Messina, R.L. Patton, R.T. Gajek, T.R. Cannan, E.M. Flanigen, Silicoaluminophosphate molecular sieves: another new class of microporous crystalline inorganic solids, *J. Am. Chem. Soc.* 106 (1984) 6092–6093.
- [66] R. Martínez-Franco, M. Moliner, Y. Yun, J. Sun, W. Wan, X. Zou, A. Corma, Synthesis of an extra-large molecular sieve using proton sponges as organic structure-directing agents, *Proc. Natl. Acad. Sci. Unit. States Am.* 110 (2013) 3749–3754.
- [67] N. Dumont, Z. Gabelica, E.G. Derouane, L.B. McCusker, Characterization and Rietveld refinement of the large pore molecular sieve SAPO-40, *Microporous Mater.* 1 (1993) 149–160.